

Rethinking Dense Cells for Integrated Sensing and Communications: A Stochastic Geometric View

Abdelhamid Salem, *Member, IEEE*, Kaitao Meng, *Member, IEEE*, Christos Masouros, *Senior Member, IEEE*, Fan Liu, *Member, IEEE*, and David Lopez-Perez, *Senior Member, IEEE*

Abstract

The inclusion of the sensing functionality in the coming generations of cellular networks, necessitates a rethink of dense cell deployments. In this paper, we analyze and optimize dense cell topologies for dual-functional radar-communication (DFRC) cellular networks. With the aid of tools from stochastic geometry, we derive new analytical expressions of the potential area spectral efficiencies in ($\text{bit}/\text{sec}/m^2$) of radar and communication systems. Based on the new formulations of the potential area spectral efficiencies, the energy efficiency (bit/Joule) of DFRC systems is provided in a closed-form formula. Then, an optimization problem to obtain the optimal base station (BS) density that maximizes the network-level energy efficiency is formulated and investigated. In this regard, the mathematical expression of the energy efficiency is shown to be a uni-modal and pseudo-concave function in the density of the BSs. Therefore, the optimal density of the BSs that maximizes the energy efficiency can be obtained. Our analytical and numerical results demonstrate that the inclusion of the sensing functionality clearly differentiates the optimal BS topologies for the DFRC systems against classical communication-only systems.

Index Terms

Multi-user MIMO, stochastic geometry, energy efficiency, integrated sensing and communications.

I. INTRODUCTION

Next-generation wireless networks will involve much more beyond communications, to provide new functionalities including sensing, localization, and activity detection. The integration of sensing and

Abdelhamid Salem, Kaitao Meng, and Christos Masouros are with the Department of Electronic and Electrical Engineering, University College London, London, UK, (emails: {a.salem, kaitao.meng, c.masouros}@ucl.ac.uk). Abdelhamid Salem is also affiliated with Benghazi University, Benghazi, Libya. Fan Liu is with the Department of Electronic and Electrical Engineering, Southern University of Science and Technology, Shenzhen 518055, China, (e-mail: liuf6@sustech.edu.cn). David Lopez-Perez is with the Algorithm and Software Design Department, Huawei Technologies, 92100 Boulogne-Billancourt, France (e-mail: dr.david.lopez@ieee.org).

communication (ISAC) has been recognized as a key 6G technology [1]–[12]. To reduce costs and improve spectral and energy efficiencies, Dual-functional Radar-Communication (DFRC) technique has received considerable attention from both industry and academia [9], [10]. DFRC technique combines both radar sensing and wireless communications via shared use of the spectrum, hardware platform and a signal processing framework [1]–[8]. DFRC system has been widely considered in the literature. For instance, in [1] the authors considered DFRC beam-forming design to simultaneously detect the targets as a multiple-input multiple output (MIMO) radar and communicate to multiple users. To characterize the performance tradeoff between MIMO radar and multiple users communication, the authors first defined the achievable performance region of the DFRC system, then both radar-centric and communication-centric optimizations were formulated to achieve the boundary of the performance region. In [2] an exact closed-form expression for the probability of false alarm was derived, while probability of detection was approximated by assuming the signal-to-noise ratio of the reference channel is much larger than that of the surveillance channel. Further work in [3] introduced a joint transmit beamforming model for a dual-function MIMO radar and multiple communication users. The proposed dual-function system transmits the weighted sum of independent radar waveforms and communication symbols, forming multiple beams towards the radar targets and the communication users, respectively. In [4], a closed-form expression of average ambiguity function has been firstly obtained, then the authors proposed a joint optimization method to improve radar peak side lobe level influenced by communication signals. In [5] the hybrid transmit/receive beam-formers have been designed by maximizing the sum-rate under transmit power constraints and the similarity between the designed beamformer and the one that has good beam pattern properties. In [6] the authors considered the mutual information between the target reflections and the target responses for DFRC systems as the design metric. Accordingly, the authors obtained the optimal waveforms with the maximum mutual information. The authors in [7] considered a MIMO DFRC system, which senses several directions and serves multiple users. Based on an orthogonal frequency division multiplexing transmission, the design of the radiated waveforms and of the receive filters employed by the radar and the users have been investigated. [In \[13\] new integrated scheduling method of sensing, communication, and control has been presented.](#) A comprehensive survey of the research progress in the areas of radar-communication coexistence and DFRC systems with particular emphasis on application scenarios and technical approaches was presented in [8]. While the above consider DFRC systems on a link level, the literature is sparse on the network-level analysis and optimization of ISAC systems.

Nevertheless, there is an abundance of literature on the network-level performance of communication only cellular networks. In the past few years, the modeling and analysis of wireless communication networks have been considered by the mathematical tool of stochastic geometry, more precisely, by the theory of spatial point processes [14]. From the system-level point of view, it has been empirically validated that the locations of the base stations (BSs) can be modeled as points of a homogeneous Poisson point process (PPP) whose intensity coincides with the average number of BSs per unit area [14]. Motivated by this, the PPP modeling approach has been widely used to analyze the trade-off between the network spectral and energy efficiencies. In [14] the authors analyzed the energy efficiency of down-link cellular networks using stochastic geometry tools. Mathematical framework of the average spectral efficiency of multi-tier cellular networks, in which single antenna BSs have been distributed in the network according to a PPP was presented in [15]. The authors in [16] provided analytical frameworks for system-level analysis and design of up-link heterogeneous cellular networks where the locations of multiple antennas BSs modeled as points of homogeneous PPP. In addition, a novel framework based on stochastic geometry for the co-existence of aerial and terrestrial users was developed in [17], where the spatial distribution of the BSs has been assumed to follow a PPP. [Tractable framework for symbol error probability, outage probability, ergodic rate, and throughput for downlink cellular networks with different MIMO configurations based on SG approach have been provided in \[18\].](#) In [19] analytical framework to study the joint impact of the sensor and the user equipment (UE) densities, on drones detection. In [20] a new mathematical approach that relies on a PPP model for the BSs locations was introduced to evaluate the performance of down-link MIMO cellular networks. In [21] a new mathematical framework to compute the error probability of downlink cellular networks based on the PPP model for the spatial BSs locations was introduced. [New models for the coverage and rate of cellular networks have been developed in \[22\] using stochastic geometry.](#) Based on these models, mathematical expressions for the coverage probability and the mean rate have been derived. In [23] based on a stochastic geometry approach, new analytical frameworks to calculate the coverage probability and average rate of cellular networks were derived with the aid of the Gil-Pelaez inversion formula. [A general study of the energy and spectral efficiencies of cellular networks has been presented in \[24\]–\[27\].](#)

Against the state-of-the-art of research on performance evaluation of DFRC systems, in this work with the aid of tools from stochastic geometry approach, we focus our attention on system-level analysis and optimization. More specifically, by taking into account the impact of network deployments we introduce

a new mathematical framework for DFRC cellular networks. In this regard, based on potential area spectral efficiency (PSE), which is the network information rate per unit area (measured in bit/sec/m^2), the energy efficiency of the DFRC network is analyzed [22]. After that, an energy efficiency optimization problem is formulated to obtain the optimal BSs density.

It has been empirically validated that, from the system-level perspective, the locations of the BSs can be modeled as points of a homogeneous PPP, whose intensity coincides with the average number of BSs per unit area. Motivated by these results, the PPP modeling approach for the locations of the DFRC BSs can be used to design the ISAC networks. Furthermore, system-level analysis and optimization are beneficial approaches when the network designers are interested in optimizing the performance of the entire ISAC networks. They can be used to optimize the current ISAC networks, and also to develop and plan future networks. In addition, analyzing and designing ISAC networks from the energy efficiency perspective necessitate proper mathematical tools, which are different from the formulas that used for optimizing the network spectral efficiency and the energy consumption individually. This optimization problem, should be formulated in a sufficiently simple realistic manner, so that all the relevant system parameters appear explicitly.

The novel contributions of this paper are listed as follows

- 1- We introduce a new analytical framework based on SG for the analysis of both sensing and communication performance for ISAC networks;
- 2- We derive a new closed-form analytical formulation of the PSE in (bit/sec/m^2) for communication systems which depend on the density of the BSs.
- 3- We derive a new closed-form analytical expression of the PSE for radar system is derived as function of the density of the BSs. The derived expressions are in closed form, without any integrations or expectations. In addition, from these expressions we can notice the impact of the system parameters on the system performance, and can be used to optimize and design the systems by formulating optimization problems, which is the main aim of these expressions.
- 4- Based on the new formulations of the potential area spectral efficiencies, the energy efficiency (bit/Joule) of DFRC systems is provided in a closed-form formula.
- 5- An energy efficiency optimization problem is formulated to find optimal BSs density that maximizes the energy efficiency of DFRC systems.
- 6- Monte-Carlo simulations are also provided to confirm the accuracy of the analysis, and to examine,

$(\cdot)^H$ and $(\cdot)^\dagger$	Conjugate transposition, and transposition
$\mathcal{E}[\cdot]$ and $\text{diag}(\cdot)$	Average operation and diagonal of a matrix
\mathbf{H} and \mathbf{h}	Channel matrix and vector
$[\mathbf{h}]_k$ and h	Element k in vector and a scalar
$ \cdot $ and $\ \cdot\ ^2$	Absolute value and Second norm
$\mathbb{C}^{K \times N}$ and \mathbf{I}	$K \times N$ matrix, and the identity matrix
\mathbf{W}	Precoding matrix
K	Average number of the users in area A
N_t	Number of transmit antennas
N_r	Number of receive antennas
d_k	Distance between the BS and the k^{th} user
α	Path loss exponent
λ_b, λ_u and λ_r	Densities of BSs, users and targets
EE	Energy efficiency
P	Transmit power

Table I: Summary of Symbols and Notations.

and investigate the impact of several parameters on the system performance, and reveal the impact of the sensing functionality on the network-level design of the ISAC networks.

The insights revealed in this work can be summarized as follows:

1- From the energy efficiency perspective, the optimal BS density for ISAC networks is lower than that for communication-only networks, which in turn changes the BS deployment significantly. This is expected since the sensing component can effectively compensate for the potential efficiency loss in the communication systems.

2- Achieving the optimal energy efficiency, the equivalent coverage radius on average is effectively improved, e.g., for the typical 5G system that has a radius area 250 m, yields an optimum radius 162.8675 m for a communication-only cellular network changes to 199.4711 m for an ISAC cellular network.

3- In the considered interference-limited scenarios, it is more energy-efficient for ISAC networks to work in low transmit power regions, i.e., less than 35dBm. Also, the energy efficiency degrades as the height of the target increases.

This paper is organized as follows. In section II, we describe the system model. Section III derives analytical expressions for the PSE and energy efficiency of communication and radar systems. Optimal BSs density is considered in Section IV. Numerical examples and simulation results are presented and discussed in section V. Finally, Section VI outlines the main conclusions of this work.

II. SYSTEM MODEL

We consider a downlink DFRC network that is designed to serve randomly positioned communication users while at the same time providing sensing services by detecting a number of randomly positioned targets. The locations of DFRC BSs are modeled using Poisson point process (PPP) Φ_b with density λ_b . The users are also generated from an independent PPP Φ_u with density λ_u , where each user is equipped with a single antenna. Number of the users in area A has a Poisson distribution with mean $K = \lambda_u A$. In addition, the targets density is λ_r , and each target flies at an altitude of h_t [28]. The DFRC BSs are equipped with multiple antennas with N_t transmit and N_r receive antennas and each user has a single antenna, without loss of generality, it is assumed that $N_t < N_r$. For clarity, Table I summarizes the commonly used symbols and notations. Following [16], [29], [30], we rely on the following standard assumptions:

- 1) All the BSs are assumed to be active and share the same transmission bandwidth.
- 2) It is assumed that the intensity of the users is high enough ($\lambda_u \gg \lambda_b$) such that each BS will have at least one user served per channel [16], and each user is associated with the nearest BS. Thus, the BSs are fully loaded with full queues, and thus the BSs always have data to transmit. The analysis with partially loaded BSs has been postponed to future work.
- 3) The channel between the BSs and the users are Rayleigh flat fading and perfectly estimated at the BSs.
- 4) The DFRC system employs a DFRC waveform that is both a communication signal and a radar probing waveform [8].

We leverage recent results in [6] that characterize the radar mutual information, to evaluate the radar information rate performance. A relevant performance metric for the design of ISAC networks is the potential spectral efficiency (PSE), which is the network information rate per unit area (measured in bit/sec/m^2) that corresponds to the minimum signal quality for reliable transmission.

In this work, we study DFRC network deployment from a network-level perspective. The main aim is to optimize the density of BSs to maximize the energy efficiency of the network. The energy efficiency (EE) is defined as a function of the communications and sensing rates and given by

$$EE = \frac{R_c + R_r}{P_T}, \quad (1)$$

where R_c is the PSE of communication, R_r is the PSE of the radar system, and P_T is the total consumed power. Next, analytical expressions of PSE for communication, R_c , and radar, R_r , are derived.

III. PSE OF DFRC SYSTEM

Due to the stationarity and the independence of all the points in any homogeneous PPP, the performance of the typical user and typical target have the same characteristics as those of any other users and targets in the networks. Therefore, we analyze the performance of typical user/targets to represent the average performance of communication and sensing in the ISAC networks. Without loss of generality, the typical user/target is located at the origin and served by its closest BS.

As we mentioned earlier, PSE is the network information rate per unit area which can be calculated in general form by [15], [16], [22]–[24]

$$R = \lambda_b \log_2 (1 + \gamma) \Pr(\gamma_0 > \gamma), \quad (2)$$

where γ_0 is the received signal to interference and noise ratio (SINR) at the typical user in communication systems and at the BS in radar systems and γ is the SINR threshold for reliable decoding. We note that, a fixed rate per user is defined, i.e., $\log_2 (1 + \gamma)$ bits/sec/Hz, and the user is served as long as the SINR allows it. This applies to delay limited transmission where the spectral efficiency is determined by evaluating the outage probability at a fixed rate, thus the outage probability plays a pivotal role.

A. PSE of communication system

In the communication system the analysis applies to a typical user, as permissible in any homogeneous PPP according to the Slivnyak–Mecke’s theorem¹ [24]. The typical user, denoted by U_o , and located at the origin. The PSE in this case can be obtained by computing the PSE of U_o and then averaging the obtained conditional PSE with respect to all possible realizations for the locations of the BSs and users. The PSE of the communication system can be calculated by [14]

$$R_c = \lambda_b \log_2 (1 + \gamma_c) \Pr(\gamma_o > \gamma_c), \quad (3)$$

where γ_c is the threshold for reliable decoding of the communication message and γ_o is the receive SINR at the typical user U_o . Universal frequency reuse is assumed, and thus each user not only receives

¹Due to the independence between the points in PPP, conditioning on a point at x does not change the distribution of the rest of the process. This is very important theorem/property, and can be applied to any user/target in the network.

information from its home BS, but also suffers interference from all the other BSs. The typical user U_o is associated with the nearest BS b . The signal transmitted by BS b is denoted by s_b . Thus, the received signal for a typical user can be written as [14], [22], [28]

$$y_o = \sqrt{P}d_{b,o}^{-\frac{\alpha}{2}} \mathbf{h}_{b,o}^\dagger \mathbf{w}_{b,o} s_{b,o} + \underbrace{\sqrt{P}d_{b,o}^{-\frac{\alpha}{2}} \sum_{k \in \Phi_u \setminus o} \mathbf{h}_{b,o}^\dagger \mathbf{w}_{b,k} s_{b,k}}_{\text{BS } b \text{'s signals to other users}} + \underbrace{\sum_{l \in \Phi_b \setminus b} \sqrt{P}d_{l,o}^{-\frac{\alpha}{2}} \mathbf{h}_{l,o}^\dagger \mathbf{W}_l s_l}_{\text{Signals transmitted from other BSs}} + n_o, \quad (4)$$

where l and $k \in \mathbb{R}^2$, $\mathbf{h}_{i,o}$ is an $N_t \times 1$ vector denoting the small scale fading between the i^{th} BS and the MU_o user, $d_{b,o}$ is the distance between the serving BS b and MU_o user, while $d_{i,0}$ is the distance from the i^{th} BS and the MU_o user. The path loss exponent is α , the precoding vector at BS b of user k is $\mathbf{w}_{b,k}$, the total precoding matrix at BS l is \mathbf{W}_l , P is the transmit power, and n_o denotes the additive white Gaussian noise (AWGN) at the user, i.e., $n_o \sim \mathcal{CN}(0, \sigma_o^2)$. Therefore, the received SINR at the typical user U_o is given by

$$\gamma_o = \frac{P d_{b,o}^{-\alpha} \left| \mathbf{h}_{b,o}^\dagger \mathbf{w}_{b,o} \right|^2}{P d_{b,o}^{-\alpha} \sum_{k \in \Phi_u \setminus o} \left| \mathbf{h}_{b,o}^\dagger \mathbf{w}_{b,k} \right|^2 + P \sum_{l \in \Phi_b \setminus b} d_{l,o}^{-\alpha} \left\| \mathbf{h}_{l,o}^\dagger \mathbf{W}_l \right\|^2 + \sigma_o^2}. \quad (5)$$

Applying zero-forcing (ZF) precoding, the pseudo-inverse of the downlink channel at the BS b is,

$$\mathbf{F}_b = \mathbf{H}_b^H (\mathbf{H}_b \mathbf{H}_b^H)^{-1} = [\mathbf{f}_{b,k}]_{1 \leq k \leq u}, \quad (6)$$

where \mathbf{H}_b is the channel matrix between the BS b and the users, $[\mathbf{f}_{b,k}]_k$ is the k th column in the matrix \mathbf{F}_b . The precoding vector at BS b for the typical user can be written as $\mathbf{w}_{b,o} = \frac{\mathbf{f}_{b,o}}{\|\mathbf{f}_{b,o}\|}$. Thus, the SINR expression in (5) can be written as

$$\gamma_o = \frac{P d_{o,o}^{-\alpha} \varsigma}{P \sum_{l \in \Phi_b \setminus b} d_{l,o}^{-\alpha} \left\| \mathbf{h}_{l,o}^\dagger \mathbf{W}_l \right\|^2 + \sigma_o^2}, \quad (7)$$

where $\varsigma = \frac{1}{\|\mathbf{f}_{b,o}\|^2} = \frac{1}{[(\mathbf{H}\mathbf{H}^H)^{-1}]_{o,o}}$. Using (3) and (7) the PSE of the communication system can be calculated by the expression presented in the next Theorem.

Theorem 1. *The PSE of the communication system can be evaluated by (8), as shown at the top of this*

$$\begin{aligned}
R_c = & \lambda_b \log_2 (1 + \gamma_c) 2\pi \lambda_b \sum_{i=1}^n H_i e^{r_i} r_i \\
& \times \prod_{k=0}^{\kappa-1} e^{-\left(\frac{2\pi \lambda_b (\kappa-1)!}{\Gamma(\kappa)} \left(\frac{1}{\alpha k!} \left(\beta \left(\left(\frac{r_i^{-\alpha}}{\gamma_c} - \frac{\sigma_0^2}{P} \right) \right) \right)^{\frac{-2}{\alpha}} \right) \Gamma\left(\frac{k+2}{\alpha}, \beta \left(\left(\frac{r_i^{-\alpha}}{\gamma_c} - \frac{\sigma_0^2}{P} \right) \right) \right) + \frac{\pi \lambda_b r_i^2}{\kappa} \right)} + R_i,
\end{aligned} \tag{8}$$

page, where r_i and H_i are the i^{th} zero and the weighting factor of the Laguerre polynomials, respectively, and the remainder R_i is negligible for Laguerre polynomials order $n > 15$ [31] and $\kappa = \frac{K}{N}$.

Proof: The proof is provided in Appendix A. ■

In this work, ZF precoding is applied at the BSs, and the interference from other BSs at the typical user is considered under the assumption of an MU-MIMO network operation with single-antenna users. In Appendix A, we present different approaches to derive exact and approximation expressions for the PSE in such a communication network. Firstly, we show that the exact expression can be obtained by deriving the cumulative distribution function (CDF) of the aggregated interference term. Thus, we first derive the moment generating function (MGF) of the aggregated interference term, then using the inverse Laplace transform or the Gil–Pelaez inversion theorem, we obtain the CDF of the aggregated interference term. However, the exact expression presented in (45) is complex, and does not present a tractable form. In order to obtain a simpler closed-form expression, we derive a tighter approximation, by only considering the dominant interferences. This technique has been considered in the literature, because of its simplicity and accuracy. We would like to indicate that the novelty in terms of analytical derivations in this work comes from using the joint comms-radar rate, as will be presented in the next sections.

B. PSE of radar system

In radar systems, without any loss in generality, the analysis is conducted on a tagged BS, the b th BS, as the reference. The analysis holds for a generic BS located at a generic location [16]. The PSE of radar systems can be calculated by

$$R_r = \lambda_b \log_2 (1 + \gamma_r) \Pr(\gamma_b > \gamma_r), \tag{9}$$

where γ_r is the threshold for reliable decoding and γ_b is the receive SINR at the b th BS.

Note that, the rate in radar systems has been defined in the literature. Most radar systems operate by radiating an electromagnetic signal into a region and detecting the echo returned from the reflecting targets. The nature of the echo signal provides information about the target, such as range, radial velocity, angular direction, size, shape, and so on. This signal is usually referred to as the radar waveform, and plays a key role in the accuracy, resolution, and ambiguity of radar in performing the above-mentioned tasks. In fact, the application of information theory to radar can be traced to the early 1950s when Woodward and Davies examined the use of information-theoretic principles to obtain the a posteriori radar receiver, shortly after the publication of Shannon's milestone work in information theory. Woodward and Davies give an excellent example of how one can use information theory to benefit radar system design [32]. Many researchers considered the connection between information theory and radar design problems until in 1993, Bell published his paper that suggested maximizing the mutual information between the target impulse response and the reflected radar signal to design radar waveforms. It was noticed that it is implied that the greater rate between the target impulse response (the target reflection) and the reflected signals, the better capability of radar to estimate the parameters describing the target. Radar rate is an appropriate metric to characterize the estimation accuracy of the system parameters, thus the more radar rate the better performance we can achieve [6], [33], [34].

Consider the typical target, $b \in \Phi_r$, the received signal at the served BS, i.e., b th BS, can be written as

$$\mathbf{y}_b = \sqrt{P}\mathbf{G}_b\mathbf{W}_b\mathbf{s}_b + \underbrace{\sum_{l \in \Phi_b \setminus b} \sqrt{P}d_{l,b}^{-\frac{\alpha}{2}}\mathbf{H}_{l,b}\mathbf{W}_l\mathbf{s}_l}_{\text{Interference from DL BSs}} + \mathbf{n}_b, \quad (10)$$

where \mathbf{G}_b is an $N_r \times N_t$ target response matrix at the b th BS and given by, $\mathbf{G}_b = \alpha_b \mathbf{a}(\theta_b) \mathbf{b}^T(\theta_b)$, α_b is the amplitude of the b th target which contains the round-trip path-loss and the radar cross-section of the target, $\mathbf{a}(\theta_b)$ and $\mathbf{b}^T(\theta_b)$ are the associated transmit and receive array steering vectors, respectively, and θ_b is its direction of arrival (DOA), $\mathbf{H}_{l,b}^\dagger$ is the $N_r \times N_t$ channel matrix between the l^{th} BS and b th BS, \mathbf{W}_i is the $N_t \times K$ precoding matrix at BS i , and \mathbf{n}_b is the disturbance in the receiver (accounting for the internal thermal noise, the sky noise, external disturbance, clutter, etc.) [6]. Please note that the above modeling implies an inherent assumption that the targets are line-of-sight (LoS), otherwise they are non-detectable. For simplicity, the reflection terms from the other targets in the system are assumed to be small after the receive filtering operation and thus it can be ignored without any major impact on

the system design. The radar receiver uses a filter \mathbf{w}_r to reduce the interference and noise. Then, the filtered signal can be written by

$$\begin{aligned} \mathbf{w}_r^H \mathbf{y}_b = & \sqrt{P} \mathbf{w}_r^H \mathbf{G}_b \mathbf{W}_b \mathbf{s}_b \\ & + \sum_{l \in \Phi_b \setminus b} \sqrt{P} d_{l,b}^{-\frac{\alpha}{2}} \mathbf{w}_r^H \mathbf{H}_{l,b} \mathbf{W}_l \mathbf{s}_l + \mathbf{w}_r^H \mathbf{n}_b, \end{aligned} \quad (11)$$

where $\mathbf{w}_r = \frac{\mathbf{R}^{-1} \mathbf{a}}{\mathbf{a}^H \mathbf{R}^{-1} \mathbf{a}}$, is the minimum variance distortion-less response (MVDR) beamformer, and $\mathbf{R} = \mathcal{E} \{ \tilde{\mathbf{n}} \tilde{\mathbf{n}}^H \} = \left\{ \sum_{l \in \Phi_b \setminus b} \sum_{k \in \Phi_u} P d_{l,b}^{-\alpha} \mathbf{z} \mathbf{z}^H + \mathbf{I} \sigma_b^2 \right\}$ and $\mathbf{z} = \mathbf{H}_{l,b} \mathbf{w}_{l,k}$ [35]. The expression in (11) can be simplified to

$$\tilde{y}_b = \sqrt{P} \mathbf{w}_r^H \mathbf{G}_b \mathbf{W}_b \mathbf{s}_b + \sum_{l \in \Phi_b \setminus b} \sqrt{P} d_{l,b}^{-\frac{\alpha}{2}} \mathbf{w}_r^H \mathbf{H}_{l,b} \mathbf{W}_l \mathbf{s}_l + \mathbf{w}_r^H \mathbf{n}_b. \quad (12)$$

Therefore, the output SINR of the radar system is

$$\gamma_b = \frac{|\alpha_b|^2 P \mathbf{w}_r^H \mathbf{G}_b \mathbf{W}_b \mathbf{s}_b \mathbf{s}_b^H \mathbf{W}_b^H \mathbf{G}_b^H \mathbf{w}_r}{\sum_{l \in \Phi_b \setminus b} P \mathbf{w}_r^H \mathbf{H}_{l,b} \mathbf{W}_l \mathbf{s}_l \mathbf{s}_l^H \mathbf{W}_l^H \mathbf{H}_{l,b}^H \mathbf{w}_r + \|\mathbf{w}_r^H\|^2 \sigma_b^2}. \quad (13)$$

Using (9) and (13) the PSE of the radar system can be calculated by the expression presented in the next Theorem.

Theorem 2. *The PSE of the radar system can be evaluated by*

$$\begin{aligned} R_r = & \lambda_b \log_2 (1 + \gamma_r) \left(1 - \sum_{i=0}^{N-1} \frac{4\pi \lambda_b}{i!} \sum_{n=1}^Q H_n e^{r_n} r_n \left(-\frac{\tilde{\alpha} (N-1) (\alpha-2) P \tilde{\alpha}_b r_n^{-\alpha_r}}{2\pi \lambda_b \beta r^{2-m} \gamma_r} \right)^i \right. \\ & \left. \times e^{-\left(\frac{(N-1)(\alpha-2)\alpha P \tilde{\alpha}_b r_n^{-\alpha_r}}{2\pi \lambda_b \beta r^{2-m} \gamma_r} + 2\pi \lambda_b (r_n^2 - h_t^2) \right)} + R_n \right) \end{aligned} \quad (14)$$

where r_{r_n} and H_n are the n^{th} zero and the weighting factor of the Laguerre polynomials, respectively, and the remainder R_n is negligible for $Q > 15$ [31].

Proof: The proof is provided in Appendix B in [36] due to page limitation.

Finally, the EE can be evaluated by substituting R_c in Theorem 1 and R_r in Theorem 2 into (1). ■

IV. OPTIMAL DENSITY OF BSS

In this section, we analyze whether there is an optimal and unique density of BSs in DFRC, communications-only and radar-only networks.

A. ISAC Network

In this sub-section, we consider whether there is an optimal and unique density of DFRC BSs that maximizes the energy efficiency while all the other system parameters are fixed and given. Mathematically, the optimization problem can be formulated as

$$\begin{aligned} & \max_{\lambda_b} \frac{R_c + R_r}{P_T} \\ & \text{subject to } \lambda_b \in [\lambda_b^{\min}, \lambda_b^{\max}]. \end{aligned} \quad (15)$$

Following [14], [37] we define $P_T = \lambda_b (P_{tx} + P_{circ})$ as the network power consumption which can be obtained by multiplying the average number of BSs per unit area, i.e., λ_b , and the average power consumption of a BS, which is $P_{tx} + P_{circ}$ where $P_{tx} = \frac{\bar{P}_{tx}}{\eta_{eff}}$, \bar{P}_{tx} is the power consumption due to the transmit power, η_{eff} is the efficiency of the amplifier and the antennas, P_{circ} the static (circuit) power, and $\lambda_b^{\min}, \lambda_b^{\max}$ are the minimum and maximum allowed density of the BSs, respectively. Without loss of generality, we can assume: $\lambda_b^{\min} \rightarrow 0, \lambda_b^{\max} \rightarrow \infty$. By substituting R_c in Theorem 1 and R_r in Theorem 2 in (15), and considering first-order Laguerre polynomial the optimization problem can be written in a more detailed formula according to the derived closed-form expression of communication rate and radar rate. Then, the formulated problem can be simplified to

$$\begin{aligned} & \max_{\lambda_b} \tilde{E}E \\ & \text{subject to } \lambda_b \in [\lambda_b^{\min}, \lambda_b^{\max}], \end{aligned} \quad (16)$$

$$\begin{aligned} \text{where } \tilde{E}E &= \left(a_1 \lambda_b \prod_{k=0}^{\kappa-1} e^{-\lambda_b a_{2,\kappa}} \right) / (P_{tx} + P_{circ}) + b_5 \left(1 - \lambda_b e^{-\left(\frac{b_3}{\lambda_b} + b_4 \lambda_b\right)} \sum_{i=0}^{N-1} b_{1,i} \left(-\frac{1}{\lambda_b}\right)^i b_{2,i} \right) / (P_{tx} + P_{circ}), \\ a_1 &= \log_2(1 + \gamma_c) 2\pi \mathbf{H}_1 e^{r_1} r_1, a_{2,\kappa} = \frac{2\pi(\kappa-1)!}{\Gamma(\kappa)} \left(\frac{1}{\alpha k!} \left(\beta \left(\frac{r_1^{-\alpha}}{\gamma_c} \right) \right)^{\frac{-2}{m}} \Gamma \left(\frac{k+2}{\alpha}, \beta \left(\frac{r_1^{-\alpha}}{\gamma_c} \right) \right) \right) + \frac{\pi r_1^2}{\kappa}, b_5 = \log_2(1 + \gamma_r), \\ b_{1,i} &= \frac{4\pi}{i!} \mathbf{H}_1 e^{r_1} r_1, b_{2,i} = \left(-\frac{\tilde{\alpha}(N-1)(\alpha-2)P\tilde{\alpha}_b r_1^{-\alpha r}}{2\pi\beta r^{2-m}\gamma_r} \right)^i, b_3 = \frac{(N-1)(\alpha-2)\tilde{\alpha}P\tilde{\alpha}_b r_1^{-\alpha r}}{2\pi\beta r^{2-\alpha}\gamma_r}, \text{ and } b_4 = 2\pi\lambda_b (r_{r_1}^2 - h_t^2). \end{aligned}$$

Using the identity that $\prod_{k=0}^{\kappa-1} e^{-\lambda_b a_{2,\kappa}} = e^{-\lambda_b \sum_{k=0}^{\kappa-1} a_{2,\kappa}}$, the last expression in (16) can be written as

$$\begin{aligned} & \max_{\lambda_b} \frac{a_1 \lambda_b e^{-\lambda_b a_3} + b_5 \left(1 - \lambda_b e^{-\left(\frac{b_3}{\lambda_b} + b_4 \lambda_b\right)} \sum_{i=0}^{N-1} b_{1,i} \left(-\frac{1}{\lambda_b}\right)^i b_{2,i} \right)}{(P_{tx} + P_{circ})} \\ & \text{subject to } \lambda_b \in [\lambda_b^{\min}, \lambda_b^{\max}], \end{aligned} \quad (17)$$

where $a_3 = \sum_{k=0}^{\kappa-1} a_{2,\kappa}$.

With the aid of some algebraic manipulations, we can observe that, the energy efficiency expression, i.e., the objective function, is a uni-modal and pseudo-concave function in λ_b , which can be proved in a similar approach as demonstrated in reference [14]. The optimal value of λ_b can be obtained as the unique solution of the following equation

$$\frac{\partial EE}{\partial \lambda_b} = \frac{\partial EE_c}{\partial \lambda_b} + \frac{\partial EE_r}{\partial \lambda_b} = 0. \quad (18)$$

The derivative of the energy efficiency of communication system, $EE_c = \frac{R_c}{P_T}$, with respect to λ_b is given by

$$\frac{\partial EE_c}{\partial \lambda_b} = a_1 e^{-a_3 \lambda_b} - a_1 a_3 \lambda_b e^{-a_3 \lambda_b}. \quad (19)$$

Similarly, the derivative of the energy efficiency of radar system, $EE_r = \frac{R_r}{P_T}$, with respect to λ_b is given by

$$\begin{aligned} \frac{\partial EE_r}{\partial \lambda_b} = & \frac{-\left(b_{1,i} b_{2,i} e^{-\left(\frac{b_3}{\lambda_b} + b_4 \lambda_b\right)} \lambda_b \left(1 + \left(-\left(\frac{1}{\lambda_b}\right)\right)^N \lambda_b\right)\right)}{(1 + \lambda_b)^2} \\ & + \frac{\left(b_{1,i} b_{2,i} e^{-\left(\frac{b_3}{\lambda_b} + b_4 \lambda_b\right)} \left(1 + \left(-\left(\frac{1}{\lambda_b}\right)\right)^N \lambda_b\right)\right)}{(1 + \lambda_b)} \\ & + \frac{\left(b_{1,i} b_{2,i} e^{-\left(\frac{b_3}{\lambda_b} + b_4 \lambda_b\right)} \lambda_b \left(1 + \left(-\left(\frac{1}{\lambda_b}\right)\right)^N \lambda_b\right) \left(\frac{b_3 - b_4}{\lambda_b^2}\right)\right)}{(1 + \lambda_b)} \\ & + \frac{\left(b_{1,i} b_{2,i} e^{-\left(\frac{b_3}{\lambda_b} + b_4 \lambda_b\right)} \lambda_b \left(\left(-\frac{1}{\lambda_b}\right)^N + \frac{\left(-\frac{1}{\lambda_b}\right)^{-1+N} N}{\lambda_b}\right)\right)}{(1 + \lambda_b)}. \end{aligned} \quad (20)$$

However, the expressions in (19) and (20) are complicated, and this makes (18) hard to solve. Nevertheless, finding solutions to polynomial formulas is quite easy using numerical methods, such as Newton's method. Newton's method can be explained as follows.

Let f be a differentiable function, and the derivative of f is f' . We seek a solution of $f(x) = 0$, starting from an initial estimate $x = x_1$. At the n th step, given x_n , compute the next approximation x_{n+1} by

$$x_{n+1} = x_n - \frac{f(x_n)}{f'(x_n)} \text{ and repeat.}$$

In order to compare the optimal value of BSs density of DFRC system with only communication system and only radar system, in the next subsections we derive also the optimal λ_b of only communication and radar systems.

B. Communications-only network

Firstly, the optimal λ_b of only communication system can be found by solving the equation

$$\frac{\partial EE_c}{\partial \lambda_b} = a_1 e^{-a_3 \lambda_b} - a_1 a_3 \lambda_b e^{-a_3 \lambda_b} = 0, \quad (21)$$

and

$$e^{-a_3 \lambda_b} = a_3 \lambda_b e^{-a_3 \lambda_b}. \quad (22)$$

Thus the optimal λ_b of only communication system is given by

$$\lambda_b = \frac{1}{a_3}. \quad (23)$$

C. Radar-only network

Secondly, the optimal λ_b of only radar system can be obtained by solving the equation

$$\begin{aligned} \frac{\partial EE_r}{\partial \lambda_b} &= \frac{-\left(b_{1,i} b_{2,i} e^{-\left(\frac{b_3}{\lambda_b} + b_4 \lambda_b\right)} \lambda_b \left(1 + \left(-\left(\frac{1}{\lambda_b}\right)\right)^N \lambda_b\right)\right)}{(1 + \lambda_b)^2} \\ &+ \frac{\left(b_{1,i} b_{2,i} e^{-\left(\frac{b_3}{\lambda_b} + b_4 \lambda_b\right)} \left(1 + \left(-\left(\frac{1}{\lambda_b}\right)\right)^N \lambda_b\right)\right)}{(1 + \lambda_b)} \\ &+ \frac{\left(b_{1,i} b_{2,i} e^{-\left(\frac{b_3}{\lambda_b} + b_4 \lambda_b\right)} \lambda_b \left(1 + \left(-\frac{1}{\lambda_b}\right)^N \lambda_b\right) \left(\frac{b_3}{\lambda_b^2} - b_4\right)\right)}{(1 + \lambda_b)} \\ &+ \frac{\left(b_{1,i} b_{2,i} e^{-\left(\frac{b_3}{\lambda_b} + b_4 \lambda_b\right)} \lambda_b \left(\left(-\frac{1}{\lambda_b}\right)^N + \frac{\left(-\frac{1}{\lambda_b}\right)^{-1+N} N}{\lambda_b}\right)\right)}{(1 + \lambda_b)} \\ &= 0. \end{aligned} \quad (24)$$

$$\lambda_b = \frac{b}{3a} - \frac{2^{\frac{1}{3}}(-b^2 - 3ac)}{3a \left(2b^3 + 9abc + 27a^2d + \sqrt{4(-b^2 - 3ac)^3 + (2b^3 + 9abc + 27a^2d)^2} \right)^{\frac{1}{3}}} + \frac{\left(2b^3 + 9abc + 27a^2d + \sqrt{4(-b^2 - 3ac)^3 + (2b^3 + 9abc + 27a^2d)^2} \right)^{\frac{1}{3}}}{3 \cdot 2^{\frac{1}{3}}a}. \quad (29)$$

With the aid of some algebraic manipulations, we can get

$$\frac{(-1)^N \lambda_b^2 \frac{1}{\lambda_b^N} (1 - N + \lambda_b (1 - N))}{\left(1 + (-1)^N \frac{1}{\lambda_b^N} \lambda_b \right)} \quad (25)$$

$$-\lambda_b^3 b_4 - \lambda_b^2 b_4 + \lambda_b (b_3 + 1) = -b_3.$$

In case $\lambda_b < 1$ we can get $\left(1 + (-1)^N \frac{1}{\lambda_b^N} \lambda_b \right) \simeq (-1)^N \frac{1}{\lambda_b^N} \lambda_b$. Therefore, (25) can be simplified to

$$\frac{(-1)^N \lambda_b^2 \frac{1}{\lambda_b^N} (1 - N + \lambda_b (1 - N))}{(-1)^N \frac{1}{\lambda_b^N} \lambda_b} \quad (26)$$

$$-\lambda_b^3 b_4 - \lambda_b^2 b_4 + \lambda_b (b_3 + 1) = -b_3,$$

which can be written as

$$\lambda_b^3 b_4 - \lambda_b^2 (1 - N - b_4) - \lambda_b (1 - N + b_3 + 1) - b_3 = 0, \quad (27)$$

where $b_3 = \frac{(N-1)(\alpha-2)\tilde{\alpha}P\tilde{\alpha}_b r_{r_1}^{-\alpha r}}{2\pi\beta r^{2-\alpha}\gamma_r}$ and $b_4 = 2\pi\lambda_b (r_{r_1}^2 - h_t^2)$. Last equation in (27) can be written in more general from as

$$a\lambda_b^3 - b\lambda_b^2 - c\lambda_b - d = 0, \quad (28)$$

which has solution given by (29).

In case $\lambda_b > 1$ we can get $\left(1 + (-1)^N \frac{1}{\lambda_b^N} \lambda_b \right) \simeq 1$. Therefore, (25) can be simplified to

$$(-1)^N (\lambda_b^{2-N} - N\lambda_b^{2-N} + \lambda_b^{3-N} (1 - N)) \quad (30)$$

$$-\lambda_b^3 b_4 - \lambda_b^2 b_4 + \lambda_b (b_3 + 1) = -b_3,$$

and

$$\lambda_b^3 b_4 + \lambda_b^2 b_4 - \lambda_b (b_3 + 1) - b_3 = 0, \quad (31)$$

$$\lambda_b = \frac{b}{3a} - \frac{2^{\frac{1}{3}}(-b^2 - 3ac)}{3a \left(-2b^3 - 9abc + 27a^2d + \sqrt{4(-b^2 - 3ac)^3 + (-2b^3 - 9abc + 27a^2d)^2} \right)^{\frac{1}{3}}} + \frac{\left(-2b^3 - 9abc + 27a^2d + \sqrt{4(-b^2 - 3ac)^3 + (-2b^3 - 9abc + 27a^2d)^2} \right)^{\frac{1}{3}}}{3 \cdot 2^{\frac{1}{3}}a}. \quad (33)$$

which can be written in more general form

$$a\lambda_b^3 + b\lambda_b^2 - c\lambda_b - d = 0, \quad (32)$$

which has solution given by (33).

These solutions of the BS densities presented in (29) and (33) depend on the system parameters. If there are more than one real and positive solutions, the optimal BS density is determined by plugging the solutions yielding the highest EE into EE.

V. NUMERICAL RESULTS

In this section, we present some numerical results in order to verify the accuracy of the derived analytical framework, to calculate the energy efficiency, and to show the results of the EE optimization problem as a function of the BSs density. Unless otherwise stated, the simulation setup is summarized in Table II. Monte Carlo simulations are executed by simulating several realizations, according to the PPP model, of the ISAC network and by computing the PSE and the power consumption. We have used the following methodology as in [38]. Step 1 : circular area of radius (R_A) around the origin is considered. Step 2 : number of BSs is generated following a Poisson distribution. Step 3 : The BSs are uni-formally distributed over the circular region. Step 4 : Independent channel gains are generated for each BS, user, and target. Step 5 : the SINR is computed. Step 6 : Finally, the EE is computed by repeating Step 1–Step 5 for 10^5 times, and then all the performance results of all snapshots are averaged.

In Fig. 1, we plot the energy efficiency versus the density of the BSs for different target heights: street-level targets at $h_t = 1.5m$, lower-level aerial targets at $h_t = 50m$, and higher-level aerial targets at $h_t = 200m$. The results depicted in Fig. 1 confirm the good accuracy of the derived analytical approach. In addition, these results show clearly the uni-modal and pseudo-concave shape of the energy

Parameter	Value
Monte-Carlo simulations repeated	10^5 times
Path loss exponent	2.7
The radius of the area (R_A)	250 m
Bw	20 MHz
P_{circ}	51.14 dBm
P_{tx}	43 dBm
η_{eff}	0.5
Number of transmit antennas	4
Number of receive antennas	8
The height of BS	25 m
The height of users	1.5 m
The height of street level target	1.5 m
The height of lower-level aerial target	50 m
The height of higher-level aerial target	200 m

Table II: Simulation Parameters.

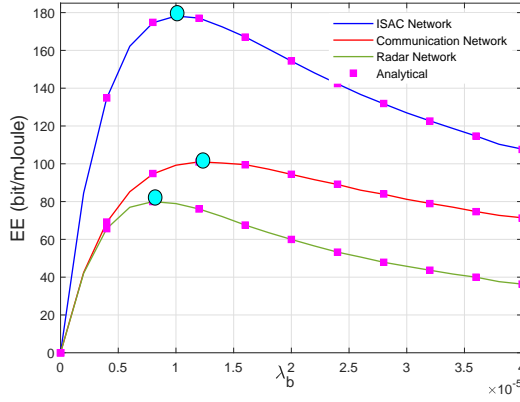
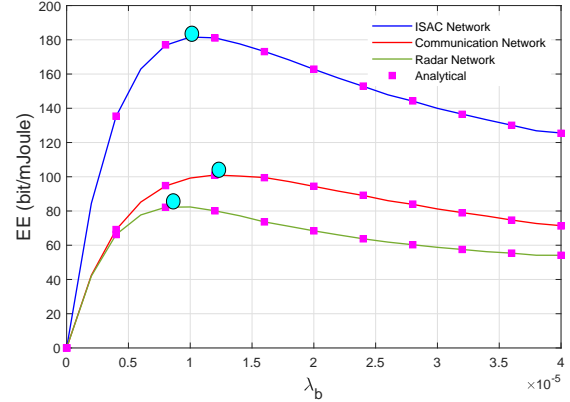
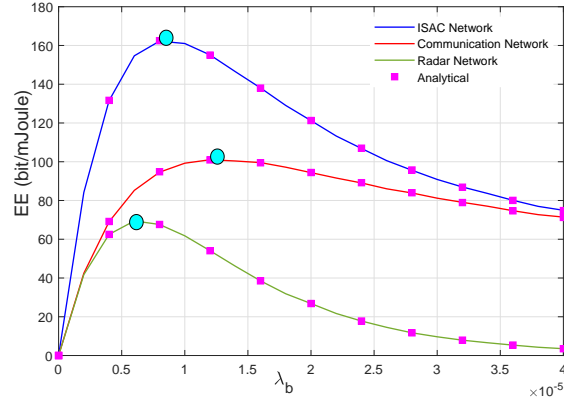
(a) Height of the target $h_t = 1.5m$.(b) Height of the target $h_t = 50m$.(c) Height of the target $h_t = 200m$.

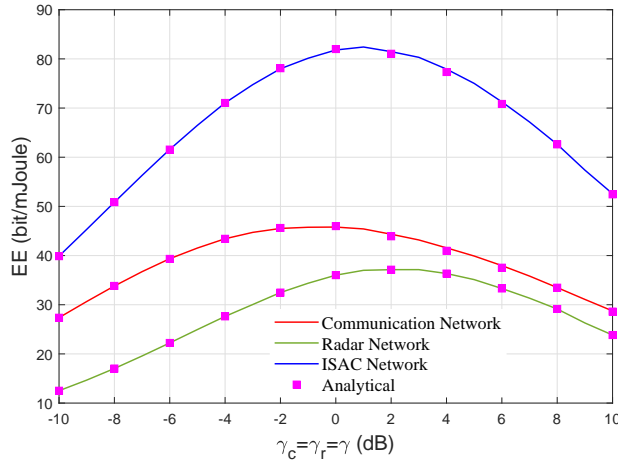
Figure 1: Energy efficiency versus the BS density for different values of the target height, the circles represent the optimal BS density.

efficiency as a function of the BSs' density for a given system parameters. Accordingly, there is an optimal value of the BSs density that maximizes the system performance. Importantly, the optimal BS density for ISAC networks is lower than that for classical communication-only networks. This is expected since the sensing component can effectively compensate for the potential efficiency loss in the communication systems. However, interestingly enough, this optimal value becomes smaller when the target altitude increases. That means, in very high altitude cases few number of BSs is adequate to reach the optimal performance due to weak interference power. Moreover, the energy efficiency performance of communication system is always better than the radar system which goes to zero as the target flies higher than 200 m for a given system set up. This is a result of the two-way propagation and hence the increased path loss experienced by the radar signal propagation.

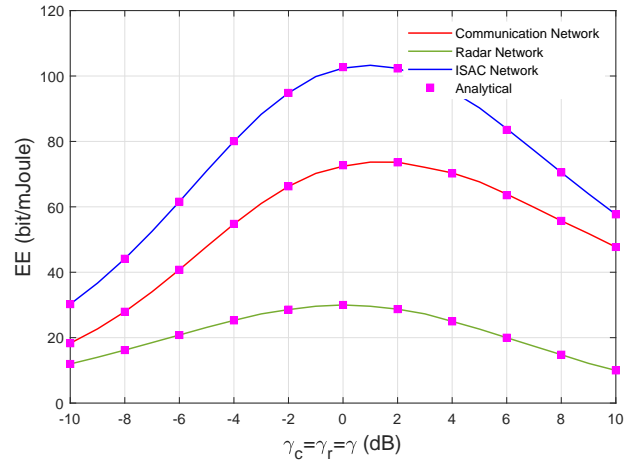
It is worth mentioning that based on the analysis in [14], [39], [40], the average cell radius can be computed as $\mathfrak{R}^c = \frac{1}{\sqrt{\pi\lambda_b}}$. Accordingly, the optimal cell radius for communication network only is $\mathfrak{R}^c = 162.8675$ m, while the optimal cell radius for ISAC network is $\mathfrak{R}^c = 178.4124$ m in street-level targets and lower-level aerial targets cases, and $\mathfrak{R}^c = 199.4711$ m in higher-level aerial targets case. The main reason is that the sensing component within the ISAC networks can effectively compensate for the potential energy efficiency loss in the communication systems under a lower BS density. As a result, ISAC networks can attain heightened energy efficiency even with lower BS density, i.e., thereby bringing a larger equivalent coverage radius.

Fig. 2 illustrates the energy efficiency versus the reliability thresholds of communication system, γ_c , and radar system, γ_r , when $\gamma_c = \gamma_r = \gamma$ for different values of the target altitude. Fig 2a presents the energy efficiency when the target altitude $h_t = 1.5$ m and Fig. 2b shows the energy efficiency when the target altitude $h_t = 50$ m. The results reveal that, the energy efficiency degrades with increasing the reliability thresholds, and there exist an optimal value of the reliability thresholds that maximizes the energy efficiency. Clearly, the optimal values for the ISAC network are distinct to the communications-only network.

In order to investigate more the impact of the reliability thresholds of communication system, γ_c , and radar system, γ_r , on the system performance, the energy efficiency is plotted in Fig. 3 with respect to γ_c and γ_r , when $\gamma_c \neq \gamma_r$ for different target heights. The energy efficiency versus γ_c when the target altitude $h_t = 1.5$ m, $\gamma_r = 2$ dB is presented in Fig 3a and when the target altitude $h_t = 50$ m, $\gamma_r = 2$ dB is shown in Fig. 3b. In addition, we plot the energy efficiency versus γ_r when the target altitude $h_t = 1.5$ m,



(a) Energy efficiency versus the reliability thresholds γ_c and γ_r when $\gamma_c = \gamma_r = \gamma$ (dB) and the height of the target $h_t = 1.5$ m.



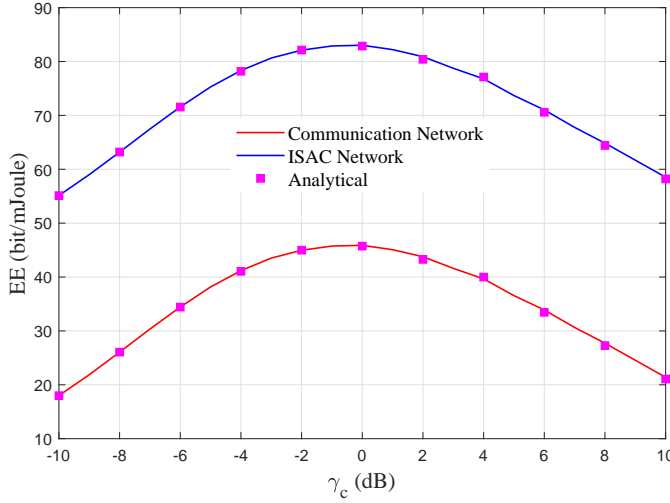
(b) Energy efficiency versus the reliability thresholds γ_c and γ_r when $\gamma_c = \gamma_r = \gamma$ (dB) and the height of the target $h_t = 50$ m.

Figure 2: Energy efficiency versus the reliability thresholds for communication, γ_c , and radar, γ_r , when $\gamma_c = \gamma_r = \gamma$ (dB) for different values of the target height.

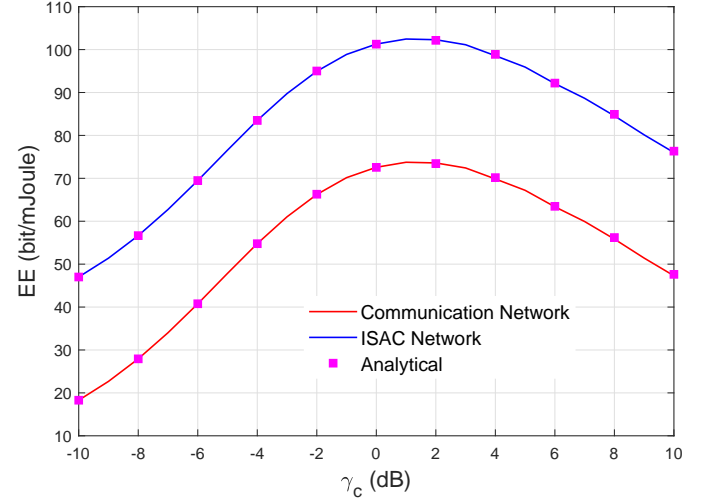
$\gamma_c = 2$ dB in Fig 3c and when the target altitude $h_t = 50$ m, $\gamma_c = 2$ dB in Fig. 3d. As we can observe from the figures that the optimal values of the reliability thresholds for communication/radar systems and DFRC system are similar, and depend on the target altitude.

To clearly demonstrate the impact of the transmit power on the system performance, we plot in Fig. 4 the energy efficiency versus P_{tx} for different values of h_t . The good matching between the analytical and simulation results again confirms the accuracy of the analysis in this paper. It is evident from these results that the energy efficiency is flat in low and medium transmit power values up to 35 dBm. However, the energy efficiency degrades sharply in high transmit power values when $P_{tx} > 35$ dBm and goes to zero in very high P_{tx} values $P_{tx} > 60$ dBm. Accordingly, all P_{tx} values up to 35 dBm are optimal and there is no a unique optimal P_{tx} value. **This can be justified by the fact that in the considered scenario the interference power is much higher than the noise power, and thus the noise power can be neglected. Indeed this fact leads to eliminate the impact of P_{tx} on the SINR expression based on the EE definition in (1).** Last observation and as anticipated that, the energy efficiency degrades as the height of the target increases.

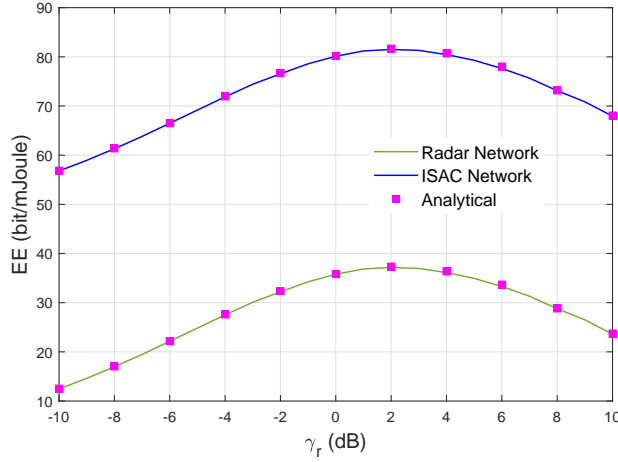
Finally, Fig. 5 depicts a 3D surface plot for the energy efficiency as a function of the target height h_t and the radius of the area R_A for radar system and DFRC system. The common observation one can see in the two systems is that the energy efficiency is at its minimum when R_A and h_t are large.



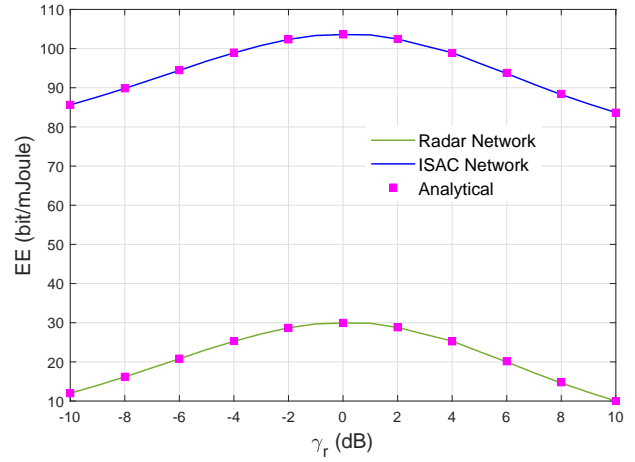
(a) Energy efficiency versus the reliability threshold for communication, γ_c , when $\gamma_r = 2$ dB and $h_t = 1.5m$.



(b) Energy efficiency versus the reliability threshold for communication, γ_c , when $\gamma_r = 2$ dB and $h_t = 50m$.



(c) Energy efficiency versus the reliability threshold for radar, γ_r , when $\gamma_c = 2$ dB and $h_t = 1.5m$.



(d) Energy efficiency versus the reliability threshold for radar, γ_r , when $\gamma_c = 2$ dB and $h_t = 50m$.

Figure 3: Energy efficiency versus the reliability thresholds for communication, γ_c , and radar, γ_r , when $\gamma_c \neq \gamma_r$ for different values of the target height.

This is because increasing the area R_A results in increasing number of BSs which leads to increase the interference power. In addition, when the target is far away from the BS, the received signal will be too weak due to larger path loss.

VI. CONCLUSION

In this paper we have presented a first network level study of the design of an ISAC network, using stochastic geometry. We derived new closed form analytical expressions of the potential spectral efficiency of communication and radar networks. Then the new derived expressions of the PSE have

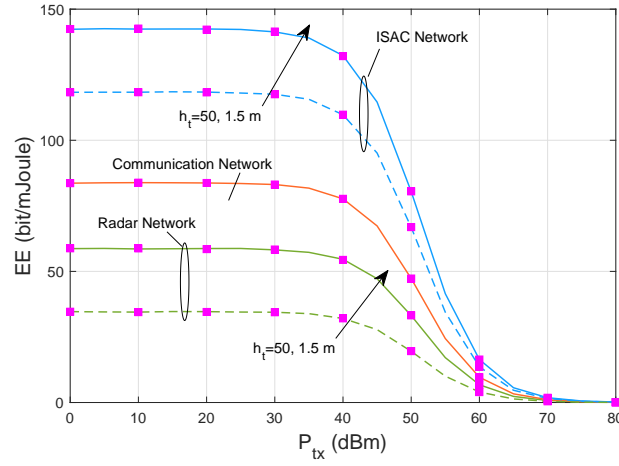


Figure 4: Energy efficiency versus the transmit power for different values of the target height.

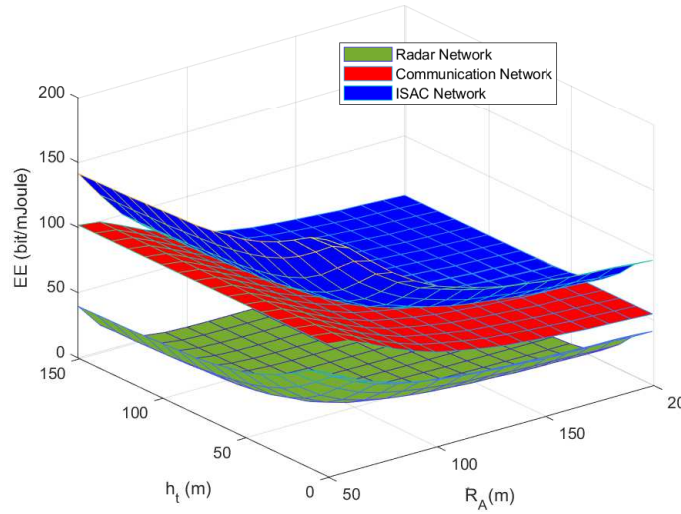


Figure 5: Energy efficiency of radar and DFRC systems versus the area radius and the target height.

been applied to the analysis and optimization of the energy efficiency of DFRC networks. Numerical results were presented to confirm our analysis and to prove the usefulness of the proposed framework for optimizing the network planning and deployment of DFRC networks. It has been proved that, the network design changes with the inclusion of the sensing functionality. The optimal DFRC BS density for the ISAC network is different to the classical communications-only network, and this optimal value becomes smaller when the target altitude increases. Therefore, few number of BSs is enough to achieve the optimal performance in very high altitude cases. The study in this work can be extended to design ISAC networks with optimal signalling and precoding schemes. In addition, the analysis can be straight forward applied to the cases when the communication users are in uplink mode. The more general cases considering the partially loaded BSs are worthwhile future works.

APPENDIX A

This appendix derives the PSE of communication system. Firstly, the coverage probability can be calculated by

$$\Pr(\gamma_o > \gamma_c) = \Pr\left(\frac{P d_{o,o}^{-\alpha} \zeta}{I_r + \sigma_o^2} > \gamma_c\right), \quad (34)$$

where $I_r = P \sum_{l \in \Phi_b \setminus b} d_{l,o}^{-m} \left\| \mathbf{h}_{l,o}^\dagger \mathbf{W}_l \right\|^2$. The expression in (34) can be written as

$$\Pr(\gamma_o > \gamma_c) = \Pr\left(I_r < \frac{P d_{o,o}^{-\alpha}}{\gamma_c} \zeta - \sigma_o^2\right), \quad (35)$$

which can be expressed as,

$$\Pr(\gamma_o > \gamma_c) = \Pr\left(\sum_{l \in \Phi_b \setminus b} d_{l,o}^{-\alpha} \left\| \mathbf{h}_{l,o}^\dagger \mathbf{W}_l \right\|^2 < \frac{d_{o,o}^{-\alpha}}{\gamma_c} \zeta - \frac{\sigma_o^2}{P}\right). \quad (36)$$

The cumulative distribution function (CDF) of I_r , can be obtained with the inverse Laplace transform.

The MGF of the aggregate interference, I_r , can be calculated by

$$\mathcal{M}_{I_r}(s) = \mathbb{E} \left\{ e^{-s \sum_{l \in \Phi_b \setminus b} d_{l,o}^{-\alpha} \left\| \mathbf{h}_{l,o}^\dagger \mathbf{W}_l \right\|^2} \right\}. \quad (37)$$

Then, the MGF can be found as

$$\mathcal{M}_{I_r}(s) = \mathbb{E}_{\Phi_b} \left\{ \prod_{l \in \Phi_b \setminus b} \mathbb{E}_{Y_l} \left\{ e^{-s d_{l,o}^{-\alpha} \left\| \mathbf{h}_{l,o}^\dagger \mathbf{W}_l \right\|^2} \right\} \right\}. \quad (38)$$

Now, $Y_l = \left\| \mathbf{h}_{l,o}^\dagger \mathbf{W}_l \right\|^2$ has gamma distribution, i.e., $Y_l \sim \Gamma(\beta, \alpha)$, with $\beta = K, \alpha = 1$. Therefore,

$$\mathcal{M}_{I_r}(s) = \mathbb{E}_{\Phi_b} \left\{ \prod_{l \in \Phi_b \setminus b} \left(1 - \frac{s d_{l,o}^{-\alpha}}{\beta} \right)^{-\alpha} \right\}. \quad (39)$$

Using the probability generating functional (PGFL) of PPP [24], $\mathcal{M}_{I_r}(s)$ can be expressed as

$$\mathcal{M}_{I_r}(s) = \exp \left(-\lambda_b \pi \int_d^r \left(1 - \left(1 - \frac{s \gamma_c u^{-\frac{\alpha}{2}}}{\beta} \right)^{-\tilde{\alpha}} \right) du \right), \quad (40)$$

which can be found as

$$\mathcal{M}_{I_r}(s) = \exp \left(-\lambda_b \left(-d + r + d {}_2F_1 \left[\alpha, -\frac{2}{\alpha}, \frac{-2 + \alpha}{\alpha}, \frac{s d^{-\alpha/2}}{\beta} \right] \right) \right)$$

$$-r_2 F_1 \left[\alpha, -\frac{2}{\alpha}, \frac{-2 + \alpha}{\alpha}, \frac{sr^{-\alpha/2}}{\beta} \right] \Bigg) \Bigg) . \quad (41)$$

If the MGF is invertible, the CDF can be found as [41], [42]

$$F(x) = \frac{1}{2\pi j} \int_{a-j\infty}^{a+j\infty} \mathcal{M}_x(s) e^{sx} ds, \quad (42)$$

where $\mathcal{M}_x(s)$ is the MGF of x . which has been simplified in [41], [42] to

$$\begin{aligned} F_X(x) = & \frac{2^{-Q} e^{\frac{A}{2}}}{x} \sum_{q=0}^Q \binom{Q}{q} \sum_{n=0}^{N+q} \frac{(-1)^n}{\beta_n} \\ & \times \Re \left(\frac{\mathcal{M}_X \left(\frac{A + 2\pi j n}{2x} \right)}{\frac{A + 2\pi j n}{2x}} \right) + E(A, N, Q), \end{aligned} \quad (43)$$

where $j^2 = -1$, $\Re \{.\}$ denotes the real part; A , N and Q are positive integers used to control accuracy and satisfy the condition that a remainder error term $E(A, N, Q)$ is negligible compared with the first term,

$$\begin{aligned} |E(A, N, Q)| = & \frac{e^{-A}}{1 - e^{-A}} + \left| \frac{2^{-Q} e^{\frac{A}{2}}}{\gamma_M} \sum_{q=0}^Q (-1)^{N+1+q} \right. \\ & \left. \binom{Q}{q} \Re \left(\frac{\mathcal{M}_\varphi \left(\frac{A + 2\pi j (N + q + 1)}{2\gamma_M} \right)}{\frac{A + 2\pi j (N + q + 1)}{2\gamma_M}} \right) \right|, \end{aligned} \quad (44)$$

$$\beta_n = \begin{cases} 2 & n = 0 \\ 1 & n = 1, 2, \dots, N + q \end{cases},$$

By plug in (41) into (43) we can get

$$\Pr \left(\sum_{l \in \Phi_b \setminus b} d_{l,o}^{-m} \left\| \mathbf{h}_{l,o}^\dagger \mathbf{W}_l \right\|^2 < \frac{d_{o,o}^{-\alpha}}{\gamma_c} \right) = \frac{2^{-Q} e^{\frac{A}{2}}}{\frac{d_{o,o}^{-\alpha}}{\gamma_c}} \sum_{q=0}^Q \binom{Q}{q}$$

$$\sum_{n=0}^{N+Q} \frac{(-1)^n}{\beta_n} \Re \left(\frac{\mathcal{M}_{I_r} \left(\frac{A + 2\pi j n}{2 \frac{d_{o,o}^{-\alpha}}{\gamma_c}} \right)}{\frac{A + 2\pi j n}{2 \frac{d_{o,o}^{-\alpha}}{\gamma_c}}} \right) + E(A, N, Q).. \quad (45)$$

Additionally, it is worthy mentioning that, the CDF of the aggregate interference in terms of its characteristic function (CF) can be also obtained by invoking the Gil–Pelaez inversion theorem in [23]. In this case the CDF can derived by

$$F(x) = \frac{1}{2} + \frac{1}{2\pi} \int_0^\infty \frac{e^{itx} \phi(-t) - e^{-itx} \phi(t)}{it} dt, \quad (46)$$

where $\phi(t)$ is CF. However, all the aforementioned ways to derive the coverage probability are complicated and simple analytical expression of the coverage probability is hard to obtain.

In order to obtain simple closed-form expression, very tight approximation has been considered in the literature for such complicated scenarios. It is also a very popular technique because of its simplicity and accuracy. This is based on deriving the coverage probability by only considering the subset of dominant interferences. Hence we have

$$\Pr(\gamma_o > \gamma_c) = \Pr \left(I_r < \frac{P d_{o,o}^{-\alpha}}{\gamma_c} \varsigma - \sigma_o^2 \right), \quad (47)$$

and

$$\Pr \left(I_r > \frac{P d_{o,o}^{-\alpha}}{\gamma_c} \varsigma - \sigma_o^2 \right) = 1 - \Pr \left(I_r < \frac{P d_{o,o}^{-\alpha}}{\gamma_c} \varsigma - \sigma_o^2 \right). \quad (48)$$

The probability term in the right-hand side (RHS) is equal to

$$\Pr \left(I_r < \frac{P d_{o,o}^{-\alpha}}{\gamma_c} \varsigma - \sigma_o^2 \right) = \Pr(\Phi_b = \phi). \quad (49)$$

Thus to compute the probability we can observe that the event $\Pr \left(I_r < \frac{P d_{o,o}^{-\alpha}}{\gamma_c} \varsigma - \sigma_o^2 \right)$ is the same as the event $\Pr(\Phi_b = \phi)$. With this observation using the expression for the void probability of a Poisson process, the conditional probability can be written as

$$\begin{aligned}
\Pr \left(I_r < \frac{P d_{o,o}^{-m}}{\gamma_c} \varsigma - \sigma_0^2 \right) &= e^{\left(-\frac{2\pi\lambda(\kappa-1)!}{\Gamma(\kappa)} \sum_{k=0}^{\kappa-1} \frac{1}{k!} \int_{d_{o,o}}^{\infty} (e^{-\beta tr^\alpha} (\beta tr^\alpha)^k) r dr \right)} \\
&= e^{-\frac{2\pi\lambda(\kappa-1)!}{\Gamma(\kappa)} \sum_{k=0}^{\kappa-1} \frac{1}{\alpha k!} \left(\beta \left(\left(\frac{d_{o,o}^{-\alpha}}{\gamma_c} - \frac{\sigma_0^2}{P} \right) \right)^{\frac{-2}{\alpha}} \right) \times \Gamma \left(\frac{k+2}{m}, \beta \left(\left(\frac{d_{o,o}^{-\alpha}}{\gamma_c} - \frac{\sigma_0^2}{P} \right) \right) \right)}.
\end{aligned}$$

$$\begin{aligned}
&\Pr \left(I_r < \frac{P d_{o,o}^{-\alpha}}{\gamma_c} \varsigma - \sigma_o^2 \right) \\
&= e^{\left(-\int_{d_{o,o}}^{\infty} \Pr \left(|x_l|^{-\alpha} \|\mathbf{h}_{l,o}^\dagger \mathbf{W}_l\|^2 > \frac{d_{o,o}^{-\alpha}}{\gamma_c} \varsigma - \frac{\sigma_o^2}{P} \right) dx \right)} \\
&= e^{\left(-\int_{d_{o,o}}^{\infty} \Pr \left(\|\mathbf{h}_{l,o}^\dagger \mathbf{W}_l\|^2 > \left(\frac{d_{o,o}^{-\alpha}}{\gamma_c} \varsigma - \frac{\sigma_o^2}{P} \right) |x_l|^\alpha \right) dx \right)} \\
&= e^{\left(-2\pi\lambda \int_{d_{o,o}}^{\infty} \Pr \left(\|\mathbf{h}_{l,o}^\dagger \mathbf{W}_l\|^2 > tr^\alpha \right) r dr \right)}, \tag{50}
\end{aligned}$$

where $t = \left(\frac{d_{o,o}^{-m}}{\gamma_c} \varsigma - \frac{\sigma_0^2}{P} \right)$. Since $Y_l = \|\mathbf{h}_{l,o}^\dagger \mathbf{W}_l\|^2$ has gamma distribution $Y_l \stackrel{d}{\sim} \Gamma(\kappa, \beta)$, (50) can be expressed as

$$\begin{aligned}
&\Pr \left(I_r < \frac{P d_{o,o}^{-m}}{\gamma_c} \varsigma - \sigma_0^2 \right) \\
&= e^{\left(-2\pi\lambda \int_{d_{o,o}}^{\infty} \left(1 - \left(\frac{\gamma(\kappa, \beta tr^\alpha)}{\Gamma(\kappa)} \right) \right) r dr \right)} \\
&= e^{\left(-2\pi\lambda \int_{d_{o,o}}^{\infty} \left(1 - \left(1 - \frac{\Gamma(\kappa, \beta tr^\alpha)}{\Gamma(\kappa)} \right) \right) r dr \right)} \\
&= e^{\left(-2\pi\lambda \int_{d_{o,o}}^{\infty} \left(\frac{\Gamma(\kappa, \beta tr^\alpha)}{\Gamma(\kappa)} \right) r dr \right)}. \tag{51}
\end{aligned}$$

Using the fact that, $\Gamma(x, y) = (x-1)! e^{-y} \sum_{k=0}^{x-1} \frac{y^k}{k!}$, (51) can be rewritten as (52). Now by taking the average over $d_{o,o}$ we can obtain equation (52), as shown at the top of the page. Since the pdf of $d_{o,o}$ is given by $f_{d_{o,o}} = 2\pi\lambda_b r e^{-\pi\lambda r^2}$, the average in (52) can be found as (53).

This expression can be simplified using Gaussian Quadrature rules. Thus, the coverage probability can be written as (54). where r_i and H_i are the i^{th} zero and the weighting factor of the Laguerre polynomials, respectively, and the remainder R_i is negligible for $n > 15$ [31]. Finally, by substituting (54)/(47) into (3) we can find the PSE of communication system presented in Theorem 1.

$$\Pr\left(I_r < \frac{Pd_{o,o}^{-\alpha}}{\gamma_c} \varsigma - \sigma_0^2\right) = E_{d_{o,o}}\left(e^{\left(-\frac{2\pi\lambda(\kappa-1)!}{\Gamma(\kappa)} \sum_{k=0}^{\kappa-1} \frac{1}{\alpha k!} \left(\left(\beta\left(\left(\frac{d_{o,o}^{-\alpha}}{\gamma_c} - \frac{\sigma_0^2}{P}\right)\right)\right)^{\frac{-2}{\alpha}}\right) \Gamma\left(\frac{k+2}{\alpha}, \beta\left(\left(\frac{d_{o,o}^{-\alpha}}{\gamma_c} - \frac{\sigma_0^2}{P}\right)\right)\right)\right)}\right). \quad (52)$$

$$\begin{aligned} \Pr\left(I_r < \frac{Pd_{o,o}^{-\alpha}}{\gamma_c} \varsigma - \sigma_0^2\right) &= 2\pi\lambda \int_0^\infty r e^{-\pi\lambda r^2} e^{\left(-\frac{2\pi\lambda(\kappa-1)!}{\Gamma(\kappa)} \sum_{k=0}^{\kappa-1} \frac{1}{\alpha k!} \left(\beta\left(\frac{r^{-\alpha}}{\gamma_c} - \frac{\sigma_0^2}{P}\right)\right)^{\frac{-2}{\alpha}} \Gamma\left(\frac{k+2}{\alpha}, \beta\left(\frac{r^{-\alpha}}{\gamma_c} - \frac{\sigma_0^2}{P}\right)\right)\right)} dr \\ &= 2\pi\lambda \int_0^\infty r e^{-\pi\lambda r^2} \prod_{k=0}^{\kappa-1} e^{-\frac{2\pi\lambda(\kappa-1)!}{\Gamma(\kappa)} \left(\frac{1}{\alpha k!} \left(\left(\beta\left(\frac{r^{-\alpha}}{\gamma_c} - \frac{\sigma_0^2}{P}\right)\right)^{\frac{-2}{\alpha}}\right) \Gamma\left(\frac{k+2}{\alpha}, \beta\left(\frac{r^{-\alpha}}{\gamma_c} - \frac{\sigma_0^2}{P}\right)\right)\right)} dr \\ &= 2\pi\lambda \int_0^\infty r \prod_{k=0}^{\kappa-1} e^{-\left(\frac{2\pi\lambda(\kappa-1)!}{\Gamma(\kappa)} \left(\frac{\left(\beta\left(\frac{r^{-\alpha}}{\gamma_c} - \frac{\sigma_0^2}{P}\right)\right)^{\frac{-2}{\alpha}}}{\alpha k!} \Gamma\left(\frac{k+2}{\alpha}, \beta\left(\frac{r^{-\alpha}}{\gamma_c} - \frac{\sigma_0^2}{P}\right)\right)\right) + \frac{\pi\lambda r^2}{\kappa}}\right)} dr \end{aligned} \quad (53)$$

APPENDIX B

This appendix derives the PSE of radar system. Now the coverage probability of the radar system can be written as

$$\begin{aligned} \Pr(\gamma_b > \gamma_r) &= \Pr\left(\frac{\frac{|\alpha_b|^2 P \mathbf{w}_r^H \mathbf{G}_b \mathbf{W}_b \mathbf{s}_b \mathbf{s}_b^H \mathbf{W}_b^H \mathbf{G}_b^H \mathbf{w}_r}{\mathbf{w}_r^H \mathbf{w}_r}}{\sum_{l \in \Phi_b \setminus b} \frac{P \mathbf{w}_r^H \mathbf{H}_{l,b} \mathbf{W}_l \mathbf{s}_l \mathbf{s}_l^H \mathbf{W}_l^H \mathbf{H}_{l,b}^H \mathbf{w}_r}{\mathbf{w}_r^H \mathbf{w}_r} + \sigma_b^2} > \gamma_r\right) \\ &= \Pr\left(X > |\alpha_b|^{-2} \gamma_r \sum_{l \in \Phi_b \setminus b} Y_l + |\alpha_b|^{-2} P^{-1} \gamma_r \sigma_b^2\right), \end{aligned} \quad (55)$$

$$\begin{aligned} \Pr\left(I_r < \frac{Pd_{o,o}^{-\alpha}}{\gamma_c} \varsigma - \sigma_0^2\right) &= 2\pi\lambda \sum_{i=1}^n \mathbf{H}_i e^{r_i r_i} \\ &\quad - \left(\frac{2\pi\lambda(\kappa-1)!}{\Gamma(\kappa)} \left(\frac{\left(\left(\beta\left(\frac{r_i^{-\alpha}}{\gamma_c} - \frac{\sigma_0^2}{P}\right)\right)^{\frac{-2}{\alpha}}\right)}{\alpha k!} \Gamma\left(\frac{k+2}{\alpha}, \beta\left(\frac{r_i^{-\alpha}}{\gamma_c} - \frac{\sigma_0^2}{P}\right)\right)\right) + \frac{\pi\lambda r_i^2}{\kappa}\right) \\ &\quad \prod_{k=0}^{\kappa-1} e^{\quad} + R_i, \end{aligned} \quad (54)$$

where $X = \frac{\mathbf{w}_r^H \mathbf{G}_b \mathbf{W}_b \mathbf{S}_b \mathbf{S}_b^H \mathbf{W}_b^H \mathbf{G}_b^H \mathbf{w}_r}{\mathbf{w}_r^H \mathbf{w}_r}$, and $Y_l = \frac{\mathbf{w}_r^H \mathbf{H}_{l,b} \mathbf{W}_l \mathbf{S}_l \mathbf{S}_l^H \mathbf{W}_l^H \mathbf{H}_{l,b}^H \mathbf{w}_r}{\mathbf{w}_r^H \mathbf{w}_r}$. In such networks $\sum_{l \in \Phi_b \setminus b} Y_l \gg \sigma_b^2$, thus

$$\Pr(\gamma_b > \gamma_r) = \Pr\left(X > |\alpha_b|^{-2} \gamma_r \sum_{l \in \Phi_b \setminus b} Y_l\right) = 1 - \Pr\left(X < |\alpha_b|^{-2} \gamma_r \sum_{l \in \Phi_b \setminus b} Y_l\right). \quad (56)$$

From the properties of wishart and inverse-wishart distributions, it has been shown that $\mathbf{W}_b \mathbf{S}_b \mathbf{W}_b^H \xrightarrow[d]{\approx} \sum_{j=1}^n \lambda_j \mathbf{I} \mathbf{W}_{b,j}$, where $\xrightarrow[d]{\approx}$ denotes the approximated distribution, λ_j is the j^{th} non-zero eigenvalues of \mathbf{S}_b and $\mathbf{I} \mathbf{W}_{b,j}$ are independent non-central inverse Wishart ($\mathbf{I} \mathbf{W}$), in case \mathbf{S}_b has one eigenvalue we can obtain, $\mathbf{W}_b \mathbf{S}_b \mathbf{W}_b^H \xrightarrow[d]{\approx} \lambda \mathbf{I} \mathbf{W}_b$ [43]–[46]. Accordingly, for non zero vector \mathbf{z} we can get $\frac{\mathbf{z}^H \mathbf{W}_b \mathbf{S}_b \mathbf{W}_b^H \mathbf{z}}{\mathbf{z}^H \mathbf{z}} \xrightarrow[d]{\approx}$ inverseGamma. Therefore, by conditioning on α_b , $X = \frac{\mathbf{w}_r^H \mathbf{G}_b \mathbf{W}_b \mathbf{S}_b \mathbf{S}_b^H \mathbf{W}_b^H \mathbf{G}_b^H \mathbf{w}_r}{\|\mathbf{I}(N, K) \mathbf{S} \mathbf{I}(K, N)\|_F \mathbf{w}_r^H \mathbf{w}_r}$, has inverse gamma(N_t, α) distribution. Similarly Y has inverse gamma(N_t, β) distribution. Thus,

$$\Pr(\gamma_b > \gamma_r) = 1 - \Pr\left(X < |\alpha_b|^{-2} \gamma_r \sum_{l \in \Phi_b \setminus b} Y_l\right) = 1 - \Pr(X < |\alpha_b|^{-2} \gamma_r y), \quad (57)$$

where $y = \sum_{l \in \Phi_b \setminus b} Y_l$. Since, X has inverse gamma($N_t, \tilde{\alpha}$) distribution, by conditioning on y we can write

$$\Pr(\gamma_b > \gamma_r) = 1 - \frac{\Gamma\left(N, \frac{\tilde{\alpha}}{|\alpha_b|^{-2} \gamma_r y}\right)}{\Gamma(N)} = 1 - \frac{\Gamma(N) - \gamma\left(N, \frac{\tilde{\alpha}}{|\alpha_b|^{-2} \gamma_r y}\right)}{\Gamma(N)} = -\frac{\gamma\left(N, \frac{\tilde{\alpha}}{|\alpha_b|^{-2} \gamma_r y}\right)}{\Gamma(N)}. \quad (58)$$

Using the series expression of Gamma function, (58) can be expressed as

$$\Pr(\gamma_b > \gamma_r) = \left(1 - e^{-\frac{\tilde{\alpha}}{\gamma_r y |\alpha_b|^{-2}}} \sum_{i=0}^{N-1} \frac{\left(\frac{\tilde{\alpha}}{|\alpha_b|^{-2} \gamma_r y}\right)^i}{i!}\right), \quad (59)$$

and thus

$$\Pr(\gamma_b < \gamma_r) = e^{-\frac{\tilde{\alpha}}{\gamma_r y |\alpha_b|^{-2}}} \sum_{i=0}^{N-1} \frac{\left(\frac{\tilde{\alpha}}{|\alpha_b|^{-2} \gamma_r y}\right)^i}{i!}. \quad (60)$$

Now by taking the average over y we can write,

$$\Pr(\gamma_b < \gamma_r) = \sum_{i=0}^{N-1} \frac{\left(\frac{\tilde{\alpha}}{\gamma_r |\alpha_b|^{-2}}\right)^i}{i!} \mathbf{E}_{\frac{1}{y}} \left[\left(\frac{1}{y}\right)^i e^{-\frac{\tilde{\alpha}}{\gamma_r y |\alpha_b|^{-2}}} \right] = \sum_{i=0}^{N-1} \frac{(s)^i}{i!} \mathbf{E}_{\frac{1}{y}} \left[\left(\frac{1}{y}\right)^i e^{-\frac{s}{y}} \right], \quad (61)$$

where $s = \frac{\tilde{\alpha}}{\gamma_r |\alpha_b|^{-2}}$. Following the property of the Laplace transform, we have, $E_v [x^n e^{-sv}] = (-1)^n \frac{d^n}{ds^n} \mathcal{L}_v(s)$, assuming $v = \frac{1}{y}$,

$$\Pr(\gamma_b < \gamma_r) = \sum_{i=0}^{N-1} \frac{(-s)^i}{i!} \frac{d^i}{ds^i} \mathcal{L}_v(s), \quad (62)$$

where $\mathcal{L}_v(s) = E_v \left[e^{-\frac{s}{y}} \right]$ and can be found as $\mathcal{L}_v(s) = E_v \left[e^{-\frac{s}{\sum_{l \in \Phi_b \setminus b} Y_l}} \right]$, using Jensen inequality we can get approximation simple closed form $\mathcal{L}_v(s) \triangleq e^{-\frac{s}{E_{\Phi, y} \left[\sum_{l \in \Phi_b \setminus b} Y_l \right]}}$. Following from the i.i.d. distribution of y_l and its further independence from the point process Φ , and applying Campbell's theory, the Laplace transform can be obtained as

$$\begin{aligned} \mathcal{L}_v(s) &\triangleq e^{-\frac{s}{E_{\Phi} \left[\sum_{l \in \Phi_b \setminus b} E[y_l] \right]}} \triangleq e^{-\frac{s}{2\pi\lambda_b \int_r \left(\int_0^\infty y_l f_{y_l}(y) dy \right) v dv}} = e^{-\frac{s}{2\pi\lambda_b \int_r \frac{\beta |v|^{-\tilde{\alpha}}}{N-1} v dv}} \\ &\triangleq e^{-\frac{s}{2\pi\lambda_b \frac{\beta r^{2-\tilde{\alpha}}}{(N-1)(\tilde{\alpha}-2)}}} = e^{-\frac{(N-1)(\tilde{\alpha}-2)s}{2\pi\lambda_b \beta r^{2-\tilde{\alpha}}}}. \end{aligned} \quad (63)$$

Now we can write the probability in (62) as

$$\Pr(\gamma_b < \gamma_r) = \sum_{i=0}^{N-1} \frac{(-s)^i}{i!} \frac{d^i}{ds^i} e^{-\frac{(N-1)(\tilde{\alpha}-2)s}{2\pi\lambda_b \beta r^{2-\tilde{\alpha}}}}, \quad (64)$$

which can be found as

$$\Pr(\gamma_b < \gamma_r) = \sum_{i=0}^{N-1} \frac{\left(-\frac{\alpha}{\gamma_r |\alpha_b|^{-2}} \right)^i}{i!} \left(-\frac{(N-1)(\tilde{\alpha}-2)}{2\pi\lambda_b \beta r^{2-\tilde{\alpha}}} \right)^i e^{-\frac{(N-1)(\tilde{\alpha}-2) \frac{\alpha}{\gamma_r |\alpha_b|^{-2}}}{2\pi\lambda_b \beta r^{2-\tilde{\alpha}}}}, \quad (65)$$

and

$$\Pr(\gamma_b > \gamma_r) = 1 - \sum_{i=0}^{N-1} \frac{1}{i!} \left(-\frac{\alpha(N-1)(\tilde{\alpha}-2)|\alpha_b|^2}{2\pi\lambda_b \beta r^{2-\tilde{\alpha}} \gamma_r} \right)^i e^{-\frac{(N-1)(\tilde{\alpha}-2)\alpha|\alpha_b|^2}{2\pi\lambda_b \beta r^{2-\tilde{\alpha}} \gamma_r}}. \quad (66)$$

The parameter α_b is the reflection coefficient, which represents the effects of both the radar path-loss and cross-section of the target, thus it can be written as $|\alpha_b|^2 = \tilde{\alpha}_b d_t^{-m}$ where $\tilde{\alpha}_b$ represent the effect of cross-section of the target and d_t^{-m} is the path-loss. Since the distance between a point in \mathbf{R}^2 and the nearest BS is distributed as $f(x) = 2\pi\lambda x e^{-2\pi\lambda x^2}$. The distance between the served BS and the typical target can be written as $d_t = \sqrt{r_t^2 + h_t^2}$ where r_t is the horizontal distance and h_t is the vertical distance. The distribution of the distance between the served BS and the typical target, d_t , for a given altitude can be derived as

$$F_{d_t}(r_r) = \Pr\left(\sqrt{r_t^2 + h_t^2} < r\right) \quad (67)$$

$$\Pr\left(\sqrt{r_t^2 + h_t^2} < r\right) = \Pr\left(r_t^2 + h_t^2 < r^2\right) = \Pr\left(r_t < \sqrt{r^2 - h_t^2}\right) = 1 - e^{-2\pi\lambda_b(r^2 - h_t^2)}. \quad (68)$$

Thus we can find

$$F_{d_t}(r) = 1 - e^{-2\pi\lambda_b(r^2 - h_t^2)} \text{ and } f_{d_t}(r) = 4r\pi\lambda_b e^{-2\pi\lambda_b(r^2 - h_t^2)}. \quad (69)$$

Now, the coverage probability can be evaluated by taking the average over the distance, d_t , thus (66) can be expressed as

$$\begin{aligned} \Pr(\gamma_b > \gamma_r) = 1 - \sum_{i=0}^{N-1} \frac{4\pi\lambda_b}{i!} \int_0^\infty r \left(-\frac{\tilde{\alpha}(N-1)(\alpha-2)P_b\tilde{\alpha}_b r^{-\alpha_r}}{2\pi\lambda_b\beta r^{2-\alpha}\gamma_r} \right)^i \\ \times e^{-\left(\frac{(N-1)(\alpha-2)\alpha P_b\tilde{\alpha}_b r^{-\alpha_r}}{2\pi\lambda_b\beta r^{2-\alpha}\gamma_r} + 2\pi\lambda_b(r^2 - h_t^2)\right)} dr_r. \end{aligned} \quad (70)$$

This expression can be simplified using Gaussian Quadrature rules to

$$\begin{aligned} \Pr(\gamma_b > \gamma_r) = 1 - \sum_{i=0}^{N-1} \frac{4\pi\lambda_b}{i!} \sum_{n=1}^Q H_n e^{r_n} r_n \left(-\frac{\tilde{\alpha}(N-1)(\alpha-2)P_b\tilde{\alpha}_b r_n^{-\alpha_r}}{2\pi\lambda_b\beta r^{2-\alpha}\gamma_r} \right)^i \\ \times e^{-\left(\frac{(N-1)(\alpha-2)\alpha P_b\tilde{\alpha}_b r_n^{-\alpha_r}}{2\pi\lambda_b\beta r^{2-\alpha}\gamma_r} + 2\pi\lambda_b(r_n^2 - h_t^2)\right)} + R_n, \end{aligned} \quad (71)$$

where r_n and H_n are the n^{th} zero and the weighting factor of the Laguerre polynomials, respectively, and the remainder R_n is negligible for $Q > 15$ [31]. Finally, by substituting (52) into (9) we can find the PSE of radar system presented in Theorem 2.

REFERENCES

- [1] L. Chen, Z. Wang, Y. Du, Y. Chen, and F. Richard Yu, "Generalized transceiver beamforming for DFRC with MIMO radar and mu-mimo communication," *IEEE Journal on Selected Areas in Communications*, pp. 1–1, 2022.
- [2] B. K. Chalise, M. G. Amin, and B. Himed, "Performance tradeoff in a unified passive radar and communications system," *IEEE Signal Processing Letters*, vol. 24, no. 9, pp. 1275–1279, 2017.
- [3] X. Liu, T. Huang, N. Shlezinger, Y. Liu, J. Zhou, and Y. C. Eldar, "Joint transmit beamforming for multiuser MIMO communications and MIMO radar," *IEEE Transactions on Signal Processing*, vol. 68, pp. 3929–3944, 2020.
- [4] L. Tang, K. Zhang, H. Dai, P. Zhu, and Y.-C. Liang, "Analysis and optimization of ambiguity function in radar-communication integrated systems using MPSK-DSSS," *IEEE Wireless Communications Letters*, vol. 8, no. 6, pp. 1546–1549, 2019.
- [5] Z. Cheng, Z. He, and B. Liao, "Hybrid beamforming for multi-carrier dual-function radar-communication system," *IEEE Transactions on Cognitive Communications and Networking*, vol. 7, no. 3, pp. 1002–1015, 2021.

- [6] B. Tang and J. Li, "Spectrally constrained MIMO radar waveform design based on mutual information," *IEEE Transactions on Signal Processing*, vol. 67, no. 3, pp. 821–834, 2019.
- [7] J. Johnston, L. Venturino, E. Grossi, M. Lops, and X. Wang, "MIMO OFDM dual-function radar-communication under error rate and beampattern constraints," *IEEE Journal on Selected Areas in Communications*, pp. 1–1, 2022.
- [8] F. Liu, C. Masouros, A. P. Petropulu, H. Griffiths, and L. Hanzo, "Joint radar and communication design: Applications, state-of-the-art, and the road ahead," *IEEE Transactions on Communications*, vol. 68, no. 6, pp. 3834–3862, 2020.
- [9] F. Liu, Y. Cui, C. Masouros, J. Xu, T. X. Han, Y. C. Eldar, and S. Buzzi, "Integrated sensing and communications toward dual functional wireless networks for 6G and beyond," *IEEE Journal on Selected Areas in Communications*, vol. 40, no. 6, pp. 1728–1767, 2022.
- [10] J. A. Zhang, F. Liu, C. Masouros, R. W. Heath, Z. Feng, L. Zheng, and A. Petropulu, "An overview of signal processing techniques for joint communication and radar sensing," *IEEE Journal of Selected Topics in Signal Processing*, vol. 15, no. 6, pp. 1295–1315, 2021.
- [11] K. Meng, Q. Wu, S. Ma, W. Chen, K. Wang, and J. Li, "Throughput maximization for UAV-enabled integrated periodic sensing and communication," *IEEE Transactions on Wireless Communications*, vol. 22, no. 1, pp. 671–687, 2023.
- [12] I. Valiulahi, C. Masouros, A. Salem, and F. Liu, "Antenna selection for energy-efficient dual-functional radar-communication systems," *IEEE Wireless Communications Letters*, vol. 11, no. 4, pp. 741–745, 2022.
- [13] B. Chang, W. Tang, X. Yan, X. Tong, and Z. Chen, "Integrated scheduling of sensing, communication, and control for mmwave/thz communications in cellular connected uav networks," *IEEE Journal on Selected Areas in Communications*, vol. 40, no. 7, pp. 2103–2113, 2022.
- [14] M. Di Renzo, A. Zappone, T. T. Lam, and M. Debbah, "System level modeling and optimization of the energy efficiency in cellular networks a stochastic geometry framework," *IEEE Transactions on Wireless Communications*, vol. 17, no. 4, pp. 2539–2556, 2018.
- [15] M. D. Renzo, A. Guidotti, and G. E. Corazza, "Average rate of downlink heterogeneous cellular networks over generalized fading channels: A stochastic geometry approach," *IEEE Transactions on Communications*, vol. 61, no. 7, pp. 3050–3071, 2013.
- [16] M. Di Renzo and P. Guan, "Stochastic geometry modeling and system-level analysis of uplink heterogeneous cellular networks with multi-antenna base stations," *IEEE Transactions on Communications*, vol. 64, no. 6, pp. 2453–2476, 2016.
- [17] W. K. New, C. Y. Leow, K. Navaie, Y. Sun, and Z. Ding, "Interference-aware noma for cellular-connected UAVs: Stochastic geometry analysis," *IEEE Journal on Selected Areas in Communications*, vol. 39, no. 10, pp. 3067–3080, 2021.
- [18] L. H. Afify, H. ElSawy, T. Y. Al-Naffouri, and M.-S. Alouini, "A unified stochastic geometry model for MIMO cellular networks with retransmissions," *IEEE Transactions on Wireless Communications*, vol. 15, no. 12, pp. 8595–8609, 2016.
- [19] P. Sinha, I. GEven, and M. C. GErsoy, "Fundamental limits on detection of UAVs by existing terrestrial rf networks," *IEEE Open Journal of the Communications Society*, vol. 2, pp. 2111–2130, 2021.
- [20] M. Di Renzo and W. Lu, "Stochastic geometry modeling and performance evaluation of MIMO cellular networks using the equivalent-in-distribution (EiD)-based approach," *IEEE Transactions on Communications*, vol. 63, no. 3, pp. 977–996, 2015.
- [21] M. Di Renzo and P. Guan, "A mathematical framework to the computation of the error probability of downlink mimo cellular networks by using stochastic geometry," *IEEE Transactions on Communications*, vol. 62, no. 8, pp. 2860–2879, 2014.
- [22] J. G. Andrews, F. Baccelli, and R. K. Ganti, "A tractable approach to coverage and rate in cellular networks," *IEEE Transactions on Communications*, vol. 59, no. 11, pp. 3122–3134, 2011.
- [23] M. Di Renzo and P. Guan, "Stochastic geometry modeling of coverage and rate of cellular networks using the gil-pelaez inversion theorem," *IEEE Communications Letters*, vol. 18, no. 9, pp. 1575–1578, 2014.

- [24] S. Mukherjee, *Analytical Modeling of Heterogeneous Cellular Networks: Geometry, Coverage, and Capacity*. Cambridge Univ. UK, Feb 2014.
- [25] W. Sun, S. Lian, H. Zhang, and Y. Zhang, "Lightweight digital twin and federated learning with distributed incentive in air-ground 6g networks," *IEEE Transactions on Network Science and Engineering*, vol. 10, no. 3, pp. 1214–1227, 2023.
- [26] W. Sun, P. Wang, N. Xu, G. Wang, and Y. Zhang, "Dynamic digital twin and distributed incentives for resource allocation in aerial-assisted internet of vehicles," *IEEE Internet of Things Journal*, vol. 9, no. 8, pp. 5839–5852, 2022.
- [27] W. Zhou, Y. Xu, and C. Li, "Multiobjective optimization for adaptive offloading in distributed multiuser mimo cell-free 6g networks," *IEEE Internet of Things Journal*, vol. 10, no. 9, pp. 7960–7973, 2023.
- [28] G. Hattab and D. Cabric, "Energy-efficient massive iot shared spectrum access over UAV-enabled cellular networks," *IEEE Transactions on Communications*, vol. 68, no. 9, pp. 5633–5648, 2020.
- [29] W. Lu and M. Di Renzo, "Stochastic geometry modeling and system level analysis and optimization of relay aided downlink cellular networks," *IEEE Transactions on Communications*, vol. 63, no. 11, pp. 4063–4085, 2015.
- [30] Y. Deng, L. Wang, M. El-kashlan, M. Di Renzo, and J. Yuan, "Modeling and analysis of wireless power transfer in heterogeneous cellular networks," *IEEE Transactions on Communications*, vol. 64, no. 12, pp. 5290–5303, 2016.
- [31] M. Abramowitz and I. A. Stegun, *Handbook of Mathematical Functions With Formulas, Graphs, and Mathematical Tabl*, Washington, D.C.: U.S. Dept. Commerce, 1972.
- [32] P. M. Woodward and I. Davies, "Xcii. a theory of radar information," *The London, Edinburgh, and Dublin Philosophical Magazine and Journal of Science*, vol. 41, no. 321, pp. 1001–1017, 1950.
- [33] Y. Yang and R. S. Blum, "MIMO radar waveform design based on mutual information and minimum mean-square error estimation," *IEEE Transactions on Aerospace and Electronic Systems*, vol. 43, no. 1, pp. 330–343, 2007.
- [34] —, "Minimax robust MIMO radar waveform design," *IEEE Journal of Selected Topics in Signal Processing*, vol. 1, no. 1, pp. 147–155, 2007.
- [35] Y. Gu and A. Leshem, "Robust adaptive beamforming based on interference covariance matrix reconstruction and steering vector estimation," *IEEE Transactions on Signal Processing*, vol. 60, no. 7, pp. 3881–3885, 2012.
- [36] A. Salem, C. Masouros, F. Liu, and D. López-Pérez, "Rethinking dense cells for integrated sensing and communications: A stochastic geometric view," *arXiv preprint arXiv:2212.12942*, 2022.
- [37] Z. Chen, L. Qiu, and X. Liang, "Area spectral efficiency analysis and energy consumption minimization in multi-antenna poisson distributed networks," *IEEE Transactions on Wireless Communications*, vol. 15, no. 7, pp. 4862–4874, 2016.
- [38] M. D. Renzo, A. Guidotti, and G. E. Corazza, "Average rate of downlink heterogeneous cellular networks over generalized fading channels: A stochastic geometry approach," *IEEE Transactions on Communications*, vol. 61, no. 7, pp. 3050–3071, 2013.
- [39] M. Di Renzo, "Stochastic geometry modeling and analysis of multi-tier millimeter wave cellular networks," *IEEE Transactions on Wireless Communications*, vol. 14, no. 9, pp. 5038–5057, 2015.
- [40] W. Lu and M. Di Renzo, "Stochastic geometry modeling of cellular networks Analysis simulation and experimental validation," in *18th ACM International Conference on Modeling, Analysis and Simulation of Wireless and Mobile Systems*, ser. Proceedings of the 18th ACM International Conference on Modeling, Analysis and Simulation of Wireless and Mobile Systems, Cancun, Mexico, Nov. 2015, pp. 179–188. [Online]. Available: <https://hal-centralesupelec.archives-ouvertes.fr/hal-01269564>
- [41] Y.-C. Ko, M.-S. Alouini, and M. Simon, "Outage probability of diversity systems over generalized fading channels," *IEEE Transactions on Communications*, vol. 48, no. 11, pp. 1783–1787, 2000.
- [42] A. Salem, L. Musavian, E. A. Jorswieck, and S. Aïssa, "Secrecy outage probability of energy-harvesting cooperative noma

transmissions with relay selection,” *IEEE Transactions on Green Communications and Networking*, vol. 4, no. 4, pp. 1130–1148, 2020.

- [43] C. R. Rao, *Linear Statistical Inference and its Applications: Second Edition*. 1973 John Wiley and Sons, 13 April 1973.
- [44] A. Meucci, *Risk and Asset Allocation*. Springer, 2005.
- [45] M. L. Eaton, *Chapter 8: The Wishart Distribution*, ser. Lecture Notes–Monograph Series. Beachwood, Ohio, USA: Institute of Mathematical Statistics, 2007, vol. Volume 53, pp. 302–333. [Online]. Available: <https://doi.org/10.1214/lnms/1196285114>
- [46] R. J. Muirhead, *Aspects of Multivariate Statistical Theory*, 1982.